

# Resonant Cavity Type Mode Transducer

SADAKUNI SHIMADA, MEMBER, IEEE

**Abstract**—This paper describes the operating principle and the properties of a resonant cavity type mode transducer which was newly devised.

The theoretical equations necessary for designing the mode transducer from a  $TE_{10}$  mode of a rectangular waveguide to an arbitrary mode of a circular waveguide have been derived, and a design method using the coupling parameters is discussed.

The experiments were made for the rectangular  $TE_{10}$ -circular  $TE_{01}$  mode transformation in the 50 Gc band. Showing an example ( $N=1$ ), the transfer loss, input SWR and mode purity were 1.34 dB, 1.13, and 95 percent (power contents), respectively, at the resonant frequency of 50 Gc/s. The 3 dB bandwidth of the transfer loss was 83 Mc/s at the constant cavity length, but it can be made much larger if the cavity length is adjusted according to the frequency change.

This mode transducer is unique in that various modes can be excited purely in the circular guide by merely varying the cavity length.

## INTRODUCTION

THREE TYPES of mode transducers, namely, a taper type, a coupled wave type, and a resonant slot type, have been used for transforming a dominant ( $TE_{10}$ ) mode of a rectangular waveguide to a certain mode of a circular waveguide [1].

The taper type transducer [2], [3] consists of a tapered waveguide whose cross section is changed from rectangular to circular so that the field of the rectangular  $TE_{10}$  mode may be transformed gradually to that of a definite circular mode. It has broadband characteristics, but the manufacturing techniques are very difficult.

The coupled wave type transducer [1], [4], [5] can be designed easily, but the manufacturing techniques are rather difficult in the millimeter wave region. Therefore, the electroforming method must be applied to it. Its frequency characteristics are narrower than those of the taper type, but broader than those of the following type.

The resonant slot type transducer [6], [7] has the advantage of a small size, but it is necessary to adjust the size of the slots experimentally at the first designing. These transducers are utilized frequently for the circular  $TE_{01}$  mode excitors in millimeter wave long-distance transmission lines.

The resonant cavity type mode transducer [8]–[12] has been newly devised and has a different operating principle from the above three transducers. Its characteristics are fundamentally the same as those of the common transmission type resonant cavity. It has the

merit of small size, but the frequency characteristics are very narrow.

Of the present three transducers, the resonant cavity type is the one most similar to the resonant slot type. The most significant difference between the two types is that the operating frequency of the resonant slot type is limited by the size of the slots, while that of the resonant cavity type is variable over a rather broad band by adjusting the cavity length.

Another merit of the resonant slot type is that it can excite various modes in the circular waveguide only by varying the cavity length.

In this paper, the operating principle and the theory of the resonant cavity type mode transducer are discussed at first. Second, as an example, the properties of the mode transformation from the rectangular  $TE_{10}$  ( $TE_{10}^{\square}$ )<sup>1</sup> to the circular  $TE_{01}$  mode ( $TE_{01}^{\circ}$ )<sup>1</sup> are investigated theoretically and experimentally.

General equations are given in the Appendix so that the mode transducer from  $TE_{10}^{\square}$  to the arbitrary  $TE_{mn}^{\circ}$  or  $TM_{mn}^{\circ}$  mode can be designed immediately. Moreover, a simple design procedure using the coupling parameters is suggested. This is also applicable to the common transmission type resonant cavity.

## OPERATING PRINCIPLE

Two fundamental structures of the resonant cavity type mode transducer are shown in Fig. 1. A cylindrical resonant cavity having a circular cross section is coupled to a rectangular guide by coupling "1," and to a circular guide by coupling "2." Figure 1(a) shows the slot cut axially in the cylindrical cavity and coupling into the end of the rectangular guide whose broad sides are parallel to the axis of the cylindrical cavity. Figure 1(b) can be obtained by rotating the rectangular guide and slot by 90 degrees.

One mode ( $TE_{10}^{\square}$ ) can propagate in the rectangular guide, while many modes can propagate in the circular guide. For an example of a  $TE_{10}^{\square}$ - $TE_{01}^{\circ}$  mode transducer, the propagating modes are at least  $TE_{11}^{\circ}$ ,  $TM_{01}^{\circ}$ ,  $TE_{21}^{\circ}$ ,  $TE_{01}^{\circ}$ , and  $TM_{11}^{\circ}$ . In fact, several other modes can propagate, because the diameter of the cavity must be enlarged in order to make the heat losses at the cavity walls smaller.

When the cavity length is chosen so that it may be resonant in a certain desired mode, the same mode as the

Manuscript received January 3, 1966; revised April 26, 1966.

The author is with Electrical Communication Laboratory, Nippon Telegraph and Telephone Public Corporation, Musasino-Si, Tokyo, Japan. He was formerly with Central Research Laboratory, Hitachi, Ltd., Tokyo, Japan.

<sup>1</sup> The rectangular and the circular modes are distinguished by the superscripts  $\square$  and  $\circ$ , respectively.

resonant one will be excited in the circular guide through coupling "2."

If the resonant mode was changed by adjusting the cavity length, another mode would be excited in the circular guide.

The varieties of the resonant modes in the cavity depend on the structure of coupling "1." In the case of the  $H_z$  coupling shown in Fig. 1(a), all  $TE^0$  modes can be coupled to the cavity, while all  $TE^0$  modes except  $TE_{0n}^0$  and all  $TM^0$  modes can be coupled in the case of the  $H_\phi$  coupling shown in Fig. 1(b).

The relation between the resonant mode and the excited mode in the circular guide depends on the shape and the distribution of the coupling holes cut in the coupling plate "2." If the many small holes are uniformly distributed as shown in Fig. 1, the same mode as the resonant one will be excited in the circular guide.

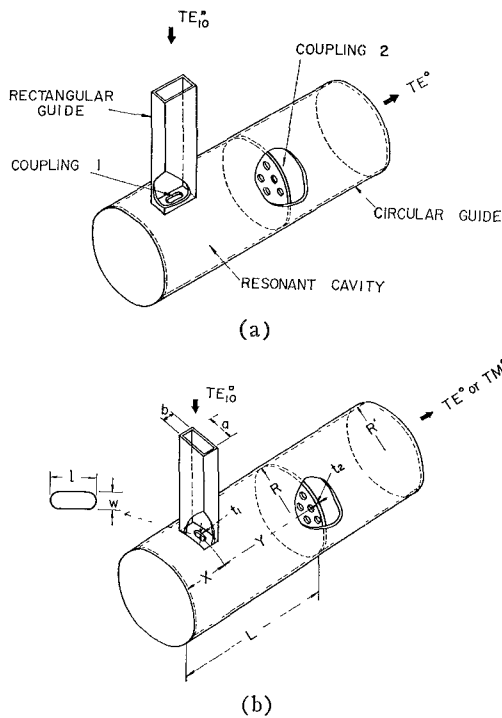


Fig. 1. Two fundamental structures of the resonant cavity type mode transducers. (a)  $H_z$  coupling. (b)  $H_\phi$  coupling.

#### THEORY AND DESIGN PROCEDURE

Generally, the following properties are desired for the mode transducer: 1) low transfer loss from  $TE_{10}^0$  to the desired mode of the circular guide, 2) small reflection coefficients, 3) broadband frequency characteristics, and 4) high mode purity.

This section includes the theoretical expressions of the half-power bandwidth and the transfer loss and input standing-wave ratio at the resonant frequency, which represent the characteristics of the resonant cavity type mode transducer. Moreover, a simple design procedure is discussed in order to obtain the ideal mode transducer.

#### *Q* Factors of the Cavity

The properties of the resonant cavity type mode transducer can be analyzed conveniently by the same theory as that of the ordinary transmission type resonant cavity, under the condition that the resonance of the main mode is not affected by the adjacent and degenerated modes in the cavity. This condition will be satisfied if the difference  $\Delta L$  between the resonant cavity lengths of the main mode and the adjacent mode is much smaller than  $L/Q_L$  ( $L$  = cavity length,  $Q_L$  = loaded  $Q$  factor of the cavity).

The loaded  $Q$  factor of the cylindrical cavity having the circular cross section is given by

$$\frac{1}{Q_L} = \frac{1}{Q_w} + \frac{1}{Q_t} + \frac{1}{Q_{e1}} + \frac{1}{Q_{e2}} \quad (1)$$

where  $Q_w$  and  $Q_t$  are caused by the heat losses at the circumference and both end plates of the cavity, respectively, while  $Q_{e1}$  and  $Q_{e2}$  are due to the coupling losses through couplings "1" and "2," respectively.

For an example of a  $TE_{10}^0$ - $TE_{01}^0$  mode transducer, the resonant mode in the cavity must be the  $TE_{01}^0$  mode.  $Q_{e1}$  and  $Q_{e2}$  mean the coupling losses from  $TE_{01}^0$  of the cavity to  $TE_{10}^0$  of the input rectangular guide through coupling "1" and from  $TE_{01}^0$  of the cavity to  $TE_{01}^0$  of the output circular guide through coupling "2," respectively.

Detailed expressions of the above four  $Q$  factors are given in the Appendix. It must be noticed that  $Q_w$  is independent of the cavity length  $L$ , but the latter three  $Q$ 's are proportional to it.

#### Half-Power Bandwidth

The half-power bandwidth of the cavity is given by

$$\Delta f = \frac{f_0}{Q_L} \quad (2)$$

where  $f_0$  is the resonant frequency.

When  $f_0$  is constant, the resonant cavity length may be written approximately by

$$L = \frac{\lambda_{g2}}{2} N \quad (N = 1, 2, 3, \dots) \quad (3)$$

where  $\lambda_{g2}$  is the guide wavelength of the resonant mode in the cavity, and  $N$  is the number of half-period variations of the field with respect to the cavity axis.

The relation between  $\Delta f$  and  $1/L$  (or  $1/N$ ) is linear, and  $\Delta f$  has the maximum value when  $N=1$ . As  $N$  grows larger,  $\Delta f$  becomes smaller, and approaches to  $f_0/Q_w$ .

#### Transfer Loss and Input Standing-Wave Ratio

The transfer loss from  $TE_{10}^0$  to a propagating mode of the circular guide may be related to the coupling parameters by

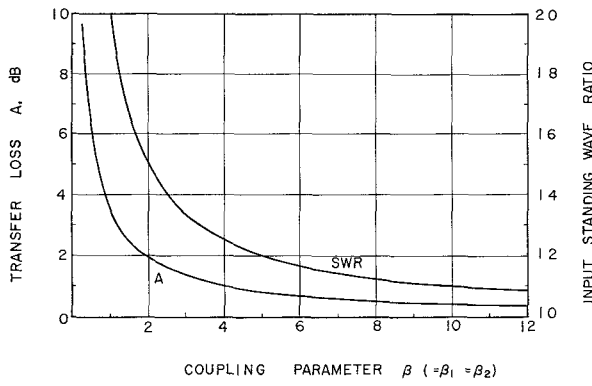


Fig. 2. Transfer loss and input SWR at the resonance vs. coupling parameter of  $\beta = \beta_1 = \beta_2$  (equal coupling).

$$A = 10 \log_{10} \frac{(1 + \beta_1 + \beta_2)^2}{4\beta_1\beta_2} \text{ dB} \quad (4)$$

$$\beta_1 = \frac{Q_0}{Q_{e1}}, \quad \beta_2 = \frac{Q_0}{Q_{e2}}, \quad Q_0 = \frac{Q_w Q_t}{Q_w + Q_t} \quad (5)$$

where  $\beta_1$  and  $\beta_2$  are the coupling parameters of couplings "1" and "2," respectively, and  $Q_0$  is equal to the unloaded  $Q$  factor of the cavity.

The input power reflection coefficient and standing-wave ratio at the resonance are

$$\Gamma = \left( \frac{1 - \beta_1 + \beta_2}{1 + \beta_1 + \beta_2} \right)^2 \quad (6)$$

$$\text{SWR} = \frac{1 + \sqrt{\Gamma}}{1 - \sqrt{\Gamma}} = \begin{cases} \frac{1 + \beta_2}{\beta_1} & (\text{when } 1 + \beta_2 \geq \beta_1) \\ \frac{\beta_1}{1 + \beta_2} & (\text{when } 1 + \beta_2 \leq \beta_1). \end{cases} \quad (7)$$

#### Design Procedure

A design method using the coupling parameters will be discussed here.

For three special cases of  $\beta_1 = \beta_2$  (equal coupling),  $\beta_1 = 1 + \beta_2$  (no input reflection), and  $\beta_2 = 1 + \beta_1$ , the transfer loss  $A$  and input SWR at the resonance vs. the coupling parameters are shown in Figs. 2 and 3. To obtain a good transducer with a low transfer loss, we must make the coupling parameters as large as possible. However, when one parameter has the upper limit, the other one must have a value larger than it by one in order to obtain the minimum transfer loss. Figure 3 corresponds to these optimum conditions, but it is preferable to select the case of  $\beta_1 = 1 + \beta_2$ , because there is no reflection at the input. To show a numerical example, the transfer loss  $A$  is 0.46 dB and the input SWR is 1.00 when  $\beta_1 = 10$  and  $\beta_2 = 9$ .

Assuming that  $\beta_1, \beta_2 \gg 1$ , namely,  $Q_0 \gg Q_{e1}, Q_{e2}$ , we can obtain from (1), (2), and (5)

$$\Delta f = f_0 \left( \frac{1}{Q_{e1}} + \frac{1}{Q_{e2}} \right). \quad (8)$$

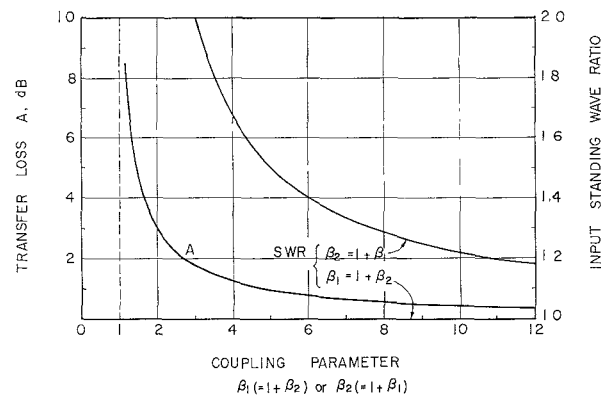


Fig. 3. Transfer loss and input SWR at the resonance vs. the coupling parameters of  $\beta_1 = 1 + \beta_2$  (no input reflection) or  $\beta_2 = 1 + \beta_1$ .

Hence small values of  $Q_{e1}$  and  $Q_{e2}$  will be desired in order to obtain the large bandwidth.

However, their values must have the proper lower limit, because it is feared that the mode purity may become worse.

#### STRUCTURE OF THE EXPERIMENTAL MODEL

Figure 4 shows an overall view of the experimental model in the 50 Gc/s band. Its detailed structure is represented by the longitudinal cross section in Fig. 5 (a). In this model the rectangular guide consists of the standard guide WRJ-500 (or WR 19), while the cavity and the circular guide have inside diameters of 12.3 mm.

This experimental model was fabricated as a universal type for the purpose of exciting some different modes in the circular guide. If it is necessary to excite only one mode, its structure can be made more simple.

Since the structure of coupling "1" corresponds to the case of  $H_z$  coupling shown in Fig. 1(a),  $\text{TM}_{11}^0$  which is degenerated with  $\text{TE}_{01}^0$  is not coupled to the cavity.

The coupling plate "2" consists of many circular holes cut in the end plate of a circular pipe with 12.3 mm OD and 11.7 mm ID. This pipe with one coupling plate was fabricated by the electroforming method and can slide smoothly in the circular guides.

As shown in Fig. 5 (a), the cavity length  $L$  is given by the sum of  $X$  and  $Y$  which can be measured with 0.001 mm units by means of a microhead and a dial gauge, respectively.

Finally, the sizes of each of the sections are arranged in the following by the same notation as that in the Appendix.

$$a = 4.78, \quad b = 2.39, \quad R = 6.15, \quad R' = 5.85$$

$$l = 2.50, \quad w = 0.80, \quad t_1 = 0.50, \quad r = 0.60, \quad t_2 = 0.30$$

$$\lambda_{g1} = 7.689 \text{ (50 Gc/s)}, \quad \lambda_{g2} = 7.457 \text{ (TE}_{01}, 50 \text{ Gc/s}),$$

$$X = \lambda_{g2}/4.$$

These dimensions are in millimeters.

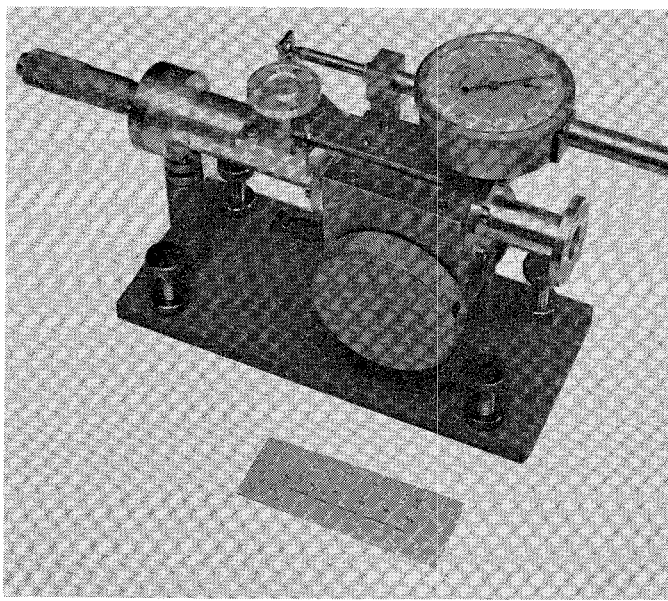


Fig. 4. Overall view of the experimental model in the 50 Gc/s band.

### EXPERIMENTAL RESULTS

We have measured the properties of the mode transformation from  $TE_{10}^{\square}$  to  $TE_{01}^{\square}$  in the previously described experimental model and compared the experimental results with the theoretical values.

#### $TE_{10}^{\square}$ - $TE_{01}^{\square}$ Transfer Loss, Input SWR, and Half-Power Bandwidth

Figure 6 shows the relation between the reciprocal of  $N$  and the half-power bandwidth  $\Delta f$  (3-dB bandwidth). Figure 7 represents the transfer loss from  $TE_{10}^{\square}$  to  $TE_{01}^{\square}$  and the input standing-wave ratio at the resonant frequency of 50 Gc/s vs.  $N=1-5$ . In these figures, the solid and the dotted lines show the theoretical values when  $\sigma=\frac{1}{4}\sigma_{dc}$  and  $\sigma=\sigma_{dc}$  ( $\sigma$ =conductivity of the plated metal on the cavity walls,  $\sigma_{dc}$ =dc conductivity of silver,  $6.17 \times 10^7 \Omega/m$ ), respectively. The measured values were used as the transmission coefficients  $T_1$  and  $T_2$  for calculation.

Referring to Figs. 6 and 7, the measured points are closer to the solid lines than the dotted lines. Therefore, it is considered that the microwave conductivity of the plated silver on the cavity walls of the experimental model may be approximately equal to a quarter of  $\sigma_{dc}$ .

The experimental values of the input SWR shown in Fig. 7 do not represent the true values, because they include the reflections from the bends and the wave-guide switch which are inserted between the standing-wave meter and the mode transducer under experiment.

The calculated values of the coupling parameters are given in table I, where the measured values of  $T_1$  and  $T_2$  (see Table II) are used for calculation. It is apparent from this table that the values of the coupling parameters have been selected improperly. If we wish to im-

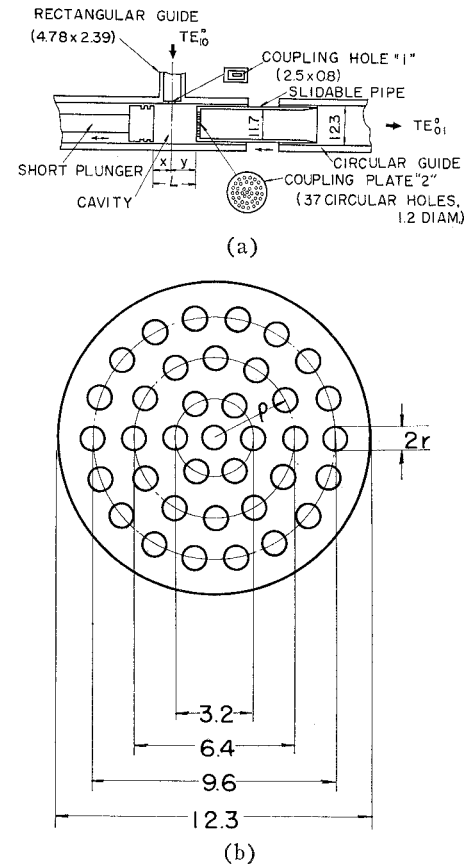


Fig. 5. (a) Longitudinal cross section of the experimental model. (b) Distributions of the circular holes in the coupling plate "2." Dimensions are in millimeters.

prove the properties of this mode transducer without largely changing the present structure, we may make the coupling "1" tighter and then get the condition of  $\beta_1=1+\beta_2$ . If  $\beta_1=4.35$  were obtained for  $N=1$ , it would be expected that the transfer loss and the input SWR would become 1.13 dB and 1.00, respectively. This improvement will reduce the transfer loss about 0.2 dB, but this difference is too small to confirm experimentally.

Table III represents the theoretical and experimental values of the resonant cavity lengths at 50 Gc/s. The theoretical values are calculated by (3), where it is assumed that the cavity is closed perfectly by the metal walls; that is, there is no coupling hole in the cavity.

The difference between the theoretical and the experimental value, which has an approximately constant value of 0.1 mm, is due to the effective susceptances of the coupling structures.<sup>2</sup>

Finally, the calculated values of all  $Q$  factors are shown in Table IV. When  $\sigma=\frac{1}{4}\sigma_{dc}$ ,  $Q_w$  and  $Q_t$  become the half values of those in Table IV, because  $Q_w$  and  $Q_t$  are proportional to  $\sqrt{\sigma}$ .

<sup>2</sup> The discussion about this difference in the former paper [10] must be corrected as described here.

### Frequency Characteristics of the Transfer Loss at the Variable Cavity Length

The resonant cavity type mode transducer has essentially the very narrow frequency characteristics at the constant cavity length. However, if the cavity length is adjusted so that the cavity may resonate constantly, the broadband properties can be obtained. Figure 8 proves this experimentally.

Though the measurements in Fig. 8 were made over the oscillation range of Klystron 50V10, this mode transducer will be useful in a broader frequency range.

### Mode Purity

In the output circular waveguide of 12.3 mm ID, twelve modes including  $TE_{01}^0$  can propagate at 50 Gc/s. Hence it is important to know the power contents of the eleven unwanted modes.

The power difference between the main  $TE_{01}^0$  mode and a certain unwanted mode was measured in dB units by means of loosely coupled mode transducers with coupling factors of  $-10$  to  $-20$  dB and the mode selectivities over 20 dB which could pick up the power of  $TE_{01}^0$  and that of a certain unwanted mode from the circular waveguide individually. These transducers used for the measurements belong to the coupled wave type and have coupling distributions according to the raised cosine function along the guide axis.

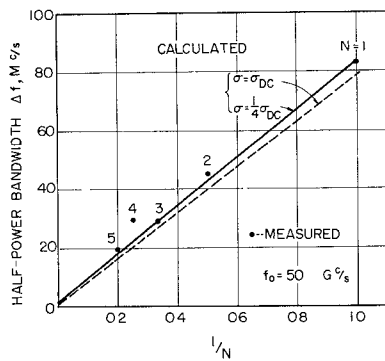


Fig. 6. Half-power bandwidth of the transfer loss from  $TE_{10}^0$  to  $TE_{01}^0$ . The resonant frequency is 50 Gc/s.

TABLE I  
THEORETICAL VALUES OF THE COUPLING PARAMETERS AT  
50 Gc/s ( $\sigma = \frac{1}{4} \sigma_{dc}$ , MEASURED VALUES OF  $T_1$  AND  $T_2$ )

$N$	$\beta_1$	$\beta_2$
1	2.88	3.35
2	2.52	2.93
3	2.24	2.61
4	2.02	2.35
5	1.84	2.14

The experimental results are shown in Table V. The power levels of eight unwanted modes are given in dB units, assuming that the power level of the  $TE_{01}^0$  mode is zero dB. The powers of the other three unwanted modes ( $TM_{02}^0$ ,  $TM_{31}^0$ , and  $TE_{51}^0$ ) have not been measured, because they will be extremely small.

Referring to Table V, the power of  $TE_{01}^0$  per all output power in the circular guide was about 95 percent. If all unwanted modes are absorbed by a proper mode filter, the power loss will correspond to about 0.2 dB.

It is apparent from the above results that the resonant cavity type mode transducer has a very good mode purity as expected.

### Excitation of Various Modes

It was previously described that the various modes could be excited in the circular guide by merely changing the cavity length. This was proved experimentally as shown in Fig. 9. The varieties of the modes excited in the circular guide could be distinguished by the resonant cavity lengths and the field patterns.

The axial magnetic fields at the circumference of the circular guide were measured by the rotary field detector, which employed a small coupling hole cut in the guide wall and could be rotated around the guide axis. Its coupling coefficient is very small, so that the fields in the guide are scarcely disturbed by the hole.

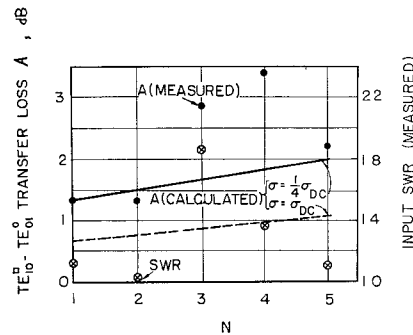


Fig. 7. Transfer loss from  $TE_{10}^0$  to  $TE_{01}^0$  and input SWR at the resonant frequency of 50 Gc/s.

TABLE II  
COUPLING COEFFICIENTS OF COUPLINGS "1" AND "2" AT 50 Gc/s

	Theoretical values	Experimental values
$T_1$	-27.00 dB	-21.87 dB
$T_2$	-22.43	-21.24

TABLE III  
RESONANT CAVITY LENGTHS AT 50 Gc/s

<i>N</i>	Theoretical values	Experimental values	Difference
1	3.729 mm	3.621 mm	0.108 mm
2	7.457	7.340	0.117
3	11.186	11.090	0.096
4	14.914	14.810	0.104
5	18.643	18.527	0.116

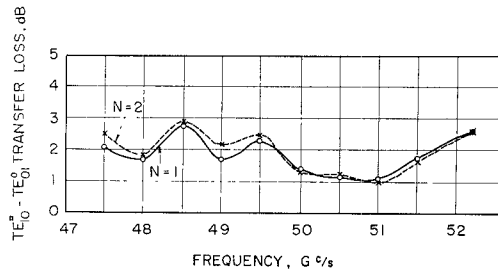


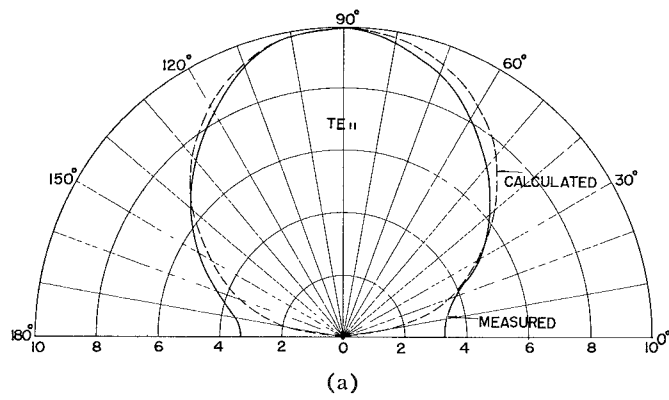
Fig. 8. Measured frequency characteristics of the transfer losses from  $TE_{10}^{\square}$  to  $TE_{01}^{\circ}$  for  $N=1$  and 2 when the cavity length is adjusted so that the cavity may resonate constantly ( $X=\lambda_{\varphi 2}/4$ ).

TABLE IV  
THEORETICAL VALUES OF *Q* FACTORS AT 50 Gc/s

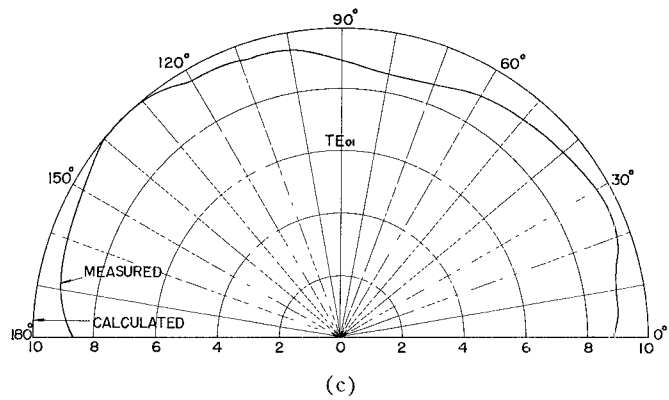
$Q_w$	$6.08 \times 10^4$	$\sigma = \sigma_{de} = 6.17 \times 10^7 \text{ V/m}$ measured values of $T_1$ and $T_2$
$Q_t$	$1.01 \times 10^4 N$	
$Q_{e1}$	$1.50 \times 10^3 N$	
$Q_{e2}$	$1.29 \times 10^3 N$	

TABLE V  
MEASURED POWER LEVELS OF THE UNWANTED MODES AT 50 Gc/s  
ASSUMING THAT THE POWER LEVEL OF THE  $TE_{01}$  MODE IS ZERO dB

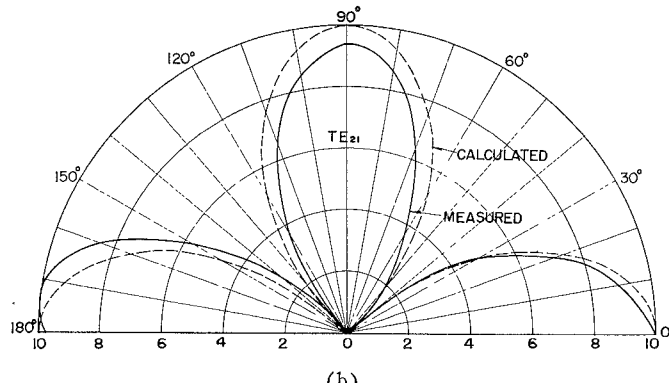
<i>N</i> Mode \	1	2	3	4	5
$TE_{11}$	-18dB	-18dB	-18dB	-17dB	-18dB
$TM_{01}$	-35	-37	-40	-28	-33
$TE_{21}$	-24	-24	-26	-28	-26
$TM_{11}$	-28	-29	-24	-18	-22
$TE_{01}$	0	0	0	0	0
$TE_{31}$	-15	-16	-16	-16	-16
$TM_{21}$	-37	-38	-39	-27	-34
$TE_{41}$	-36	-35	-33	-37	-34
$TE_{12}$	below	below	below	below	below
	-35	-35	-35	-35	-35



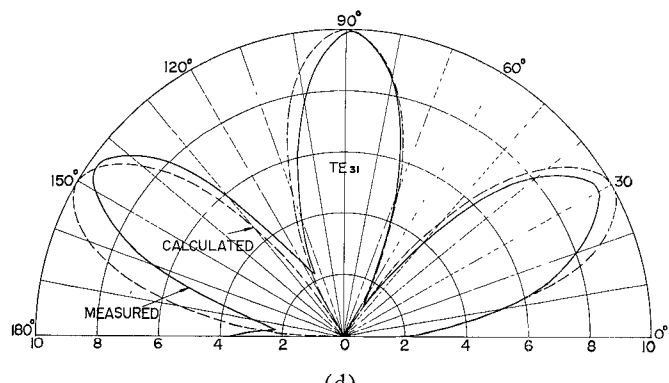
(a)



(c)



(b)



(d)

Fig. 9. Circumferential distributions of the axial magnetic fields of the circular guide wall at 50 Gc/s. [ $X=1.5$  mm,  $L=\lambda_{\varphi 2}/2$  ( $N=1$ )]. (a)  $L=3.131$ , 3.025 mm calculated, measured. (b)  $L=3.408$ , 3.318 mm. (c)  $L=3.729$ , 3.608. (d)  $L=3.958$ , 3.857.

## CONCLUSION

Resonant cavity type mode transducers can be designed by using the theoretical equations and the design method described in this paper.

However, it must be noticed that the conductivity of the cavity walls in the millimeter wave region is usually smaller than the dc conductivity, as is well known in ordinary cavities and waveguides. In the experimental model shown in this paper, it is considered that the conductivity will be nearly equal to a quarter of  $\sigma_{dc}$  at 50 Gc/s.

Showing an example of the measured properties, the transfer loss from  $TE_{10}^{\square}$  to  $TE_{01}^{\circ}$ , the input SWR, and the mode purity were 1.34 dB, 1.13, and 95 percent (power contents), respectively, at the resonant frequency of 50 Gc/s for  $N=1$ .

On the other hand, the experimental results for the coupled wave type mode transducers were 0.9 dB,<sup>3</sup> 1.05, and 92 percent at 50 Gc/s [12].

Comparing the above results for two different types of mode transducer, we find that their properties are not so different. However, the frequency characteristics are extremely dissimilar. For the former transducer the 3 dB bandwidth of the transfer loss was 83 Mc/s for  $N=1$ , and for the latter one, 0.9–1.5 dB<sup>3</sup> over the frequency range of 46–52 Gc/s [12]. Hence it is known that the frequency characteristics of the resonant cavity type transducer are very narrow, but if the cavity length is adjusted so that the cavity may resonate constantly, it will be made much broader, as shown in Fig. 8, where the transfer losses are 1.05–2.73 dB for  $N=1$  over the frequency range of 47.5–52.2 Gc/s.

Finally, we will propose an improved model of the resonant cavity type transducer from  $TE_{10}^{\square}$  to  $TE_{01}^{\circ}$  as shown in Fig. 10 to reduce the heat losses at both end plates of the cylindrical cavity.

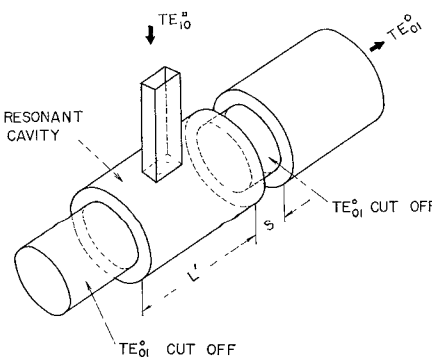


Fig. 10. An improved model of the resonant cavity type  $TE_{10}^{\square}$ - $TE_{01}^{\circ}$  mode transducer.

<sup>3</sup> The transfer losses quoted in (10) include a heat loss of about 0.5 dB in the helix waveguide (12.3 mm ID, 280 mm length) and the rectangular guide (about 200 mm length).

Two circular guides in which the  $TE_{01}^{\circ}$  mode are under cutoff are connected with both ends of the cavity. In these smaller guides, the amplitude of the  $TE_{01}^{\circ}$  mode is attenuated exponentially along the axis at the same phase; hence, the coupling coefficient between the cavity and the output circular guide can be varied by the length  $S$  of the right side small guide in Fig. 10. Of course, it is desirable for the left side one to be long enough so that the  $TE_{01}^{\circ}$  mode may not be radiated in the free space.

## APPENDIX

$Q$  factors of  $TE_{mn}^{\circ}$  and  $TM_{mn}^{\circ}$  modes in the cylindrical cavity are well known [13]:

$$Q_w = \frac{\pi \lambda_{g2}}{\lambda^2 \alpha}, \quad Q_t = \frac{\pi Z_0}{4 \Re} \left( \frac{\lambda_{g2}}{\lambda} \right)^2 N$$

$$Q_{e1} = \frac{2\pi}{T_1} \left( \frac{\lambda_{g2}}{\lambda} \right)^2 N, \quad Q_{e2} = \frac{2\pi}{T_2} \left( \frac{\lambda_{g2}}{\lambda} \right)^2 N \quad (9)$$

where

$\alpha$ =attenuation constants of the circular waveguide constructing the circumferential wall of the cavity (Neper/m)

$Z_0$ =characteristic impedance ( $377 \lambda_{g2}/\lambda$  for TE,  $377 \lambda/\lambda_{g2}$  for TM)

$\Re$ =characteristic resistance of the metal wall of the cavity

$\lambda$ =free space wavelength

$\lambda_{g2}$ =guide wavelength in the cavity

$N=2L/\lambda_{g2}$  ( $L$ =cavity length)

$T_1$  and  $T_2$ =power coupling coefficients of coupling "1" and "2."

If the sizes of coupling holes are small enough in comparison with the wavelength, the power coupling coefficients can be easily obtained by means of Bethe's theory. [14].

For the experimental model of the  $TE_{10}^{\square}$ - $TE_{01}^{\circ}$  mode transducer shown in Fig. 4,  $T_1$  and  $T_2$  are given by

$$T_1 = \frac{8}{\pi} \frac{x_{01}^2}{R^4 ab} \frac{\lambda_{g2}}{\lambda_{g1}} \sin^2 \left( \frac{2\pi}{\lambda_{g2}} X \right) M_1 10^{-d_1}$$

$$T_2 = \{ 6C_2 (\rho = 1.6 \text{ mm}) + 12C_2 (\rho = 3.2 \text{ mm}) + 18C_2 (\rho = 4.8 \text{ mm}) \}^2$$

$$C_2(\rho) = \frac{4}{J_0^2(x_{01})} \frac{1}{RR' \sqrt{\lambda_{g2} \lambda_{g2}'}} J_1 \left( \frac{\rho}{R} x_{01} \right) \cdot J_1 \left( \frac{\rho}{R'} x_{01} \right) M_2 10^{-\alpha_2/2} (x_{01} = 3.83171) \quad (10)$$

where

$\lambda_{g1}$  = guide wavelength of  $TE_{10}^{\square}$

$X$  = distance from the center of the slot to the end plate of the cavity

$$M_1 = \frac{\pi l^3}{24 \left( \log_e \frac{4l}{w} - 1 \right)},$$

$$\alpha_1 = 2.728 \frac{t_1}{l} \sqrt{1 - \left( \frac{2l}{\lambda} \right)^2}$$

$l, w$  = length and width of the slot which has an approximately elliptic shape ( $l \gg w$ )

$t_1$  = depth of the slot

$a, b$  = inner dimensions of the rectangular guide

$R$  = radius of the cavity

$R'$  = radius of the output circular guide which corresponds to the inside radius of the slidable pipe in Fig. 5(a)

$\lambda_{g2}'$  = guide wavelength in the output circular guide

$$M_2 = \frac{4}{3} r^3, \quad \alpha_2 = 3.200 \frac{t_2}{2r} \sqrt{1 - \left( 1.706 \frac{2r}{\lambda} \right)^2}$$

$r$  = radius of the circular hole in coupling plate "2"

$\rho$  = position of the circular hole [see Fig. 5(b)]

$t_2$  = depth of the circular hole.

## ACKNOWLEDGMENT

The author wishes to thank Prof. K. Suetake, Tokyo Institute of Technology, for his valuable discussions, and Dr. I. Sekiguchi, Hitachi Central Research Lab., for his constant encouragement.

## REFERENCES

- [1] B. Oguchi and K. Yamaguchi, "Centre-excited type of rectangular  $TE_{10}^{\square}$  to circular  $TE_{01}^{\square}$  mode transducer," *Proc. IEE*, vol. 106, pt. B, suppl. 13, p. 132-137, January 1959.
- [2] G. C. Southworth, *Principles and Applications of Waveguide Transmission*. Princeton, N. J.: Van Nostrand, p. 362.
- [3] P. H. Wolfert, "A wide-band rectangular-to-circular mode transducer for millimeter waves," *IEEE Trans. on Microwave Theory and Techniques (Correspondence)*, vol. MTT-11, pp. 430-431, September 1963.
- [4] S. E. Miller, "Coupled wave theory and waveguide applications," *Bell Sys. Tech. J.*, vol. 33, p. 661-719, May 1954.
- [5] A. Jaumann, "Über Richtungskoppler zur Erzeugung der  $H_{01}^{\square}$ -Welle im Runden Hohlleiter," *Arch. elekt. Übertragung*, vol. 12, p. 440-446, October 1958.
- [6] D. A. Lanciani, " $H_{01}^{\square}$  mode circular waveguide components," *IRE Trans. on Microwave Theory and Techniques*, vol. MTT-2, pp. 45-51, July 1954.
- [7] K. Noda, "Mode excitors in circular waveguides," *Rev. Elec. Commun. Lab. (Japan)*, vol. 8, p. 465-476, September-October 1960.
- [8] S. Shimada, "Resonant cavity type mode transducer," *1961 Nat'l Conv. Rec. IECE of Japan*, no. 196, November 1961.
- [9] —, "Resonant cavity type mode transducer and mode filter for the circular  $TE_{02}^{\square}$  mode," *Millimeter and Submillimeter Conf.*, Orlando, Fla., January 1963.
- [10] —, "Resonant cavity type  $TE_{10}^{\square}$ - $TE_{01}^{\square}$  mode transducer," *J. IECE of Japan*, vol. 48, p. 1206-1215, July 1965.
- [11] —, "Circular waveguide components at millimeter wavelength-mode transducers," *Hitachi, Rev. (Japan)*, to be published.
- [12] —, "Mode transducers in the 50 Gc/s region," *rept. of the research committee on millimeter waves in Japan*, pp. 62-64. Japan: Corona, 1963.
- [13] C. G. Montgomery, *Principles of Microwave Circuits*. New York: McGraw-Hill, ch. 2.
- [14] H. A. Bethe, "Theory of diffraction by small holes," *Phys. Rev.*, vol. 66, p. 163-182, 1944.

# Dispersion Characteristics of an Array of Parasitic Linear Elements

E. R. NAGELBERG, MEMBER, IEEE, AND J. SHEFER, SENIOR MEMBER, IEEE

**Abstract**—In this paper we study the properties of a transmission line consisting of an infinite array of conducting cylinders, placing emphasis on the dispersion characteristics of the lowest order slow wave mode. We present experimental results for the variation of phase velocity with frequency, and then, using a method of parameter estimation, determine the element current distribution which best explains these observations. Assuming this distribution to be of the form

$$j(x; \gamma) = j_0 \left[ 1 - \left( \frac{|x|}{h} \right)^\gamma \right],$$

Manuscript received March 18, 1966; revised May 2, 1966.  
The authors are with Bell Telephone Laboratories, Inc., Whippny, N. J.

we find that, for a given size of element, there is a value of  $\gamma$  which gives very good agreement for the variation of phase velocity over the frequency range of interest.

## I. INTRODUCTION

IN THE FOLLOWING we study certain characteristics of an infinitely long, uniform array of conducting cylinders, as illustrated in Fig. 1. This structure can support a guided wave which travels along the axis with a phase velocity less than the velocity of light. The propagation characteristics of this slow wave are of interest for two reasons. First, the results may be applied to analysis of the Yagi antenna, which can be thought of